Global stability analysis of azimuthal oscillations in Hall Thrusters

IEPC-2013-304

Presented at the 33rd International Electric Propulsion Conference,
The George Washington University, Washington, D.C., USA
October 6–10, 2013

Diego Escobar*
Universidad Politécnica de Madrid (UPM), Madrid, 28040, Spain

Eduardo Ahedo†
Universidad Carlos III de Madrid (UC3M), Leganés, 28911, Spain

This article presents results from a linearized time-dependent two-dimensional (axial and azimuthal) fluid model of the Hall thruster discharge. The model is used to carry out a global stability analysis of the plasma response, as opposed to the more commonly used local stability analysis. Experimental results indicate the existence of low frequency long wave-length azimuthal oscillations in the direction of the ExB drift, usually referred to as spokes. Our model predicts the presence of such oscillations for typical Hall thruster conditions with a frequency and growth rate similar to the breathing mode, a purely axial low frequency oscillation typical in Hall thrusters. A comparison between the simulated breathing mode and the simulated spoke shows similar features between them. Moreover, the contribution of this azimuthal oscillation to electron conductivity is evaluated by computing the equivalent anomalous diffusion coefficient from the linear oscillations. The results show a relevant contribution to anomalous diffusion in the rear part of the thruster.

Nomenclature

$_{i,e,n}$	= subindex for ion, electron and neutral species
$_{x,y}$	= subindex for axial and azimuthal coordinates
e, m_e, m_i	= electron charge and electron and ion masses
$\vec{E}, \vec{B}$	= electric and magnetic field vectors
$u_0, \tilde{u}_1$	= zero-th and first order solutions of macroscopic variable u
u_1	= coefficient of Fourier-expanded perturbation of macroscopic variable u
n, n_n	= plasma and neutral densities
$\vec{v}_j, v_{jx}, v_{jy}$	= velocity vector and axial and azimuthal velocities of species j
T_e, ϕ	= electron temperature and electric potential
ν_i, ν_e	= ionization frequency and effective electron collision frequency
ν_w, ν_{we}	= particle and energy wall-loss frequencies
α_i	= energy loss per ionization
$\omega_{i,e}$	= ion and electron cyclotron frequencies
ω, k	= angular frequency and azimuthal wave number of perturbation
χ	= Hall parameter
a_w	= wall accommodation factor

*PhD Candidate, Equipo de Propulsión Espacial y Plasmas (EP2), descobar@gmv.com
†Professor, Equipo de Propulsión Espacial y Plasmas (EP2), eduardo.ahedo@uc3m.es

I. Introduction

Hall Effect Thrusters (HET) are a type of electric propulsion device whose operation principle is as follows. A strong radial magnetic field is imposed together with an axial electric field inside a coaxial chamber where a neutral gas, typically Xenon, is introduced as propellant. Three species of particles are present in a HET: neutrals, which are injected from the rear part of the channel and flow axially towards the thruster exit; electrons, which are introduced by a cathode located just outside the channel and flow upstream towards the anode describing an **E**x**B** closed-drift in the azimuthal direction; and ions, which are created by ionization of neutrals due to collisions with the counter-streaming electrons and are accelerated axially by the electric field in the channel and the near plume. For a given thruster, the main control parameters are the discharge voltage, the magnetic field, and the mass flow rate, being the discharge current an output of the dynamical system. For a given magnetic field and mass flow rate, it is possible to represent the evolution of the discharge current as a function of the discharge voltage in the so-called current-voltage (I-V) curve. This curve shows two distinct regimes: a low ionization regime, where the discharge current increases with the voltage; and a current saturated regime, where the discharge current is fairly insensitive to changes in the discharge voltage.

Hall thrusters have now become a mature alternative to chemical propulsion in many space applications ranging from orbital raising of satellites through north-south station-keeping of geostationary satellites to low-thrust propulsion of interplanetary probes. However, not all physical processes inside Hall thrusters are fully understood, in particular, the electron conductivity. Since the early stages of the Hall thruster technology development, it has been clear that the cross-field electron mobility inside the chamber and in the plume is too high to be explained with classical collisional theories[1] . That is why the term anomalous diffusion is normally used to refer to the higher-than-expected electron axial current.

The main properties of the anomalous diffusion, experimentally verified, may be summarized as: a) it is present in the whole channel as well as in the plume of the thruster[2] ; b) it is higher outside than inside the channel[3] ; c) there is a dip of electron conductivity in the region of high magnetic and electric field;[2–5] d) the electron mobility scales as $1/B$ rather than as $1/B^2$ according to experiments[6,7] , where B is the magnetic field strength; and e) the magnetic field gradients affect greatly the electron conductivity.[8]

Currently there is no agreement within the Hall thruster community about the mechanism of the anomalous diffusion, but the most accepted explanations are two: plasma oscillations, referred to as Bohm-type or turbulent diffusion, based on the fact that correlated azimuthal oscillations of plasma density and electric field can induce a net axial electron current[9,10] ; and near-wall conductivity, where secondary electrons emitted by the walls can induce a net axial current[11] . However, near-wall conductivity does not seem to explain the anomalous diffusion due to the $1/B$ scaling suggested by Boniface *et al.*[6] . And many simulation codes[12–14] that model the near-wall conductivity still need Bohm-type diffusion to match the electron conductivity measured experimentally. On the other hand, several experiments have confirmed with various techniques the presence of *azimuthal* oscillations. These oscillations are normally grouped into low frequency (5-30 kHz), low-to-medium frequency (30-100 kHz) and high frequency (1-10 MHz) azimuthal oscillations[15] . Several experimental analyses show the presence of low frequency azimuthal oscillations originated in the rear part of the thruster[10,16–26] . The theoretical analysis of these oscillations, usually called spokes, is the topic of the present study.

This paper analyzes the stability of the Hall discharge from a global point of view, as opposed to the more widely used local stability analysis. The latter are based on the analysis of the fluid equations at a fixed axial location of the channel and need to freeze the macroscopic plasma variables and its derivatives, whereas the former do account consistently for the axial variation of those variables and of the linear perturbations. Most of the stability analyses of the Hall discharge in the azimuthal direction carried out so far are local and can be grouped in those[8,27–31] that do not account for the ionization process and those[17,32–35] that take it into consideration in the model through particle source terms and fluid equations for the neutral species. However, all these local stability studies suffer from the problems mentioned above. On the other hand, the few studies[36–40] that do account globally for the axial variations of the inhomogeneous plasma focus on the high frequency range. The current study fills the gap of global stability analyses in the low frequency range, where the ionization process plays a very important role.

The paper is organized as follows. In Section II the formulation of the linearized time-dependent two-dimensional (2D) model used in the study is presented. Section III shows and discusses the results from the model, including a parametric variation with respect to the discharge voltage and a comparison against the breathing mode. Finally, Section IV summarizes the main conclusions of the study.

II. Formulation

This section presents the formulation used in this study. Firstly, the one-dimensional (1D) model of Ahedo et al.[41] , upon which the 2D model is based, is summarized. Then, the linearised time-dependent 2D formulation is presented. Finally, the anomalous diffusion caused by the oscillations is evaluated.

A. 1D model of Ahedo

The hypotheses and equations of the 1D stationary model of Ahedo of the Hall discharge are reviewed in this section. Each one of the species present in a HET (neutrals, electrons and single-charge ions) is accounted for with a separate set of macroscopic fluid equations based on conservation principles of mass, momentum, and energy. Quasi-neutrality is assumed as the Debye length in Hall thrusters is much smaller than the length of the channel. Furthermore, whereas electrons are highly magnetized, ions are considered to be unmagnetized. On the other hand, due to the very low mass of the electrons, electron-inertia terms are neglected in the electron momentum and energy equations. At the same time, ions and neutrals are modelled as cold species. Wall energy losses and wall particle recombination are included in the model via equivalent frequencies. A sink is introduced in the energy equation to account for the ionization and radiation losses. Heat conduction is also neglected in the model. Notice that the induced magnetic field is neglected and thus, Maxwell's equations are not part of the model. The magnetic field is equal to the field externally applied, which is stationary ($\partial\vec{B}/\partial t = 0$), solenoidal ($\nabla \cdot \vec{B} = 0$), irrotational ($\nabla \times \vec{B} = 0$) and mostly radial. Consequently, the electric field derives from a potential ($\vec{E} = -\nabla\phi$). The resulting formulation may be written as:

$$\begin{aligned}
\frac{d}{dx}(nv_{ex}) = \frac{d}{dx}(nv_{ix}) &= -\frac{d}{dx}(n_n v_{nx}) = n(\nu_i - \nu_w) \\
m_i n_n v_{nx}\frac{dv_{nx}}{dx} &= m_i n \nu_w (1 - a_w)(v_{ix} - v_{nx}) \\
m_i n v_{ix}\frac{dv_{ix}}{dx} &= -en\frac{d\phi}{dx} - m_i n \nu_i (v_{ix} - v_{nx}) \\
0 &= -\frac{d}{dx}(nT_e) + en\frac{d\phi}{dx} - m_e n \nu_e \chi^2 v_{ex} \\
\frac{d}{dx}\left(\frac{5}{2}nT_e v_{ex}\right) &= env_{ex}\frac{d\phi}{dx} - n\nu_i\alpha_i - n\nu_{we}T_e
\end{aligned} \tag{1}$$

where x is the axial coordinate along the thruster channel; e, m_e, and m_i are the electron charge, electron mass, and ion mass respectively; n_n and n are the neutral and plasma particle densities; v_{nx}, v_{ex} and v_{ix} are the fluid axial velocity of neutrals, electrons and ions respectively; T_e and ϕ are the electron temperature and electric potential; ν_e, ν_i, ν_w, and ν_{we} represent the frequencies for effective electron collisions (including as well Bohm-type diffusion), ionization, particle wall recombination and energy wall losses respectively; α_i is the energy loss per actual created ion; and a_w is the accommodation factor of the ions impacting the walls. The electron azimuthal momentum equation, $v_{ey} = v_{ex}\chi$, where v_{ey} is the electron azimuthal velocity, which is negative as v_{ex}, and $\chi = eB/m_e\nu_e \gg 1$ is the Hall parameter, has been used implicitly in the axial electron momentum equation. The combination of the previous equations allows obtaining an equation for $h \equiv \ln n$ as:

$$P\frac{dh}{dx} = G \tag{2}$$

where $P = T_e/m_i - (3/5)v_{ix}^2$ and G is a function of the macroscopic variables, but not of their derivatives. Since heat conduction is not considered, the sonic point condition is $P = 0$. It is possible to proof that there are two sonic points in the domain, one singular, $G \neq 0$, in the anode sheath transition, and another one regular, $G = 0$, inside the channel. A detailed description of the boundary conditions associated to the previous system of ordinary differential equations is described by Ahedo *et al.*[41] . Expressions for the different frequencies mentioned above (ν_i, ν_e, ν_w, ν_{we}) may be found elsewhere.[12,41–43]

Various versions of the model presented above including different terms have been used to characterize the Hall discharge[41] , evaluate the influence of the wall losses[12] , carry out parametric investigations on the operating conditions[43] , model two-stage Hall thrusters[44] , and even analyze the stability of the discharge against small axial perturbations and study the properties of the breathing mode.[45–47]

B. General 2D formulation

The equations presented in the previous section can be extended to two dimensions (axial, x, and azimuthal, y) with time-dependent terms (t being the time variable). Under the same hypotheses, the governing time-dependent 2D equations of the plasma discharge may be written as:

$$\begin{aligned}
\frac{\partial n}{\partial t} + \nabla \cdot (n\vec{v}_e) = \frac{\partial n}{\partial t} + \nabla \cdot (n\vec{v}_i) = -\frac{\partial n_n}{\partial t} - \nabla \cdot (n_n \vec{v}_n) = n(\nu_i - \nu_w) \\
m_i n_n \left(\frac{\partial \vec{v}_n}{\partial t} + \vec{v}_n \cdot \nabla \vec{v}_n \right) = m_i n \nu_w (1 - a_w)(\vec{v}_i - \vec{v}_n) \\
m_i n \left(\frac{\partial \vec{v}_i}{\partial t} + \vec{v}_i \cdot \nabla \vec{v}_i \right) = -en\nabla\phi - m_i n \nu_i (\vec{v}_i - \vec{v}_n) \\
0 = -\nabla(nT_e) - en(-\nabla\phi + \vec{v}_e \times \vec{B}) - m_e n \nu_e \vec{v}_e \\
\frac{\partial}{\partial t}\left(\frac{3}{2} n T_e \right) + \nabla \cdot \left(\frac{5}{2} n T_e \vec{v}_e \right) = en\vec{v}_e \cdot \nabla\phi - n\nu_i \alpha_i - n\nu_{we} T_e
\end{aligned} \tag{3}$$

where $\vec{v}_e$, $\vec{v}_i$, and $\vec{v}_n$ are the electron, ion, and neutral velocity vectors respectively, and the rest of the symbols are as above.

It is important to remark that even though the equations above can be applied to the fully three-dimensional problem, in this case the radial variation of the variables is neglected reducing the problem to two-dimensions. Moreover, curvature effects in the azimuthal direction are also neglected as the mean radius of the channel is typically larger than the width of the channel. Obviously in the limit of a stationary and axi-symmetric solution Eqs. (3) reduce to Eqs. (1).

Equations (3) can be rewritten in a form more amenable to the current study. To this end, the partial derivatives with respect to t and y, which will be Fourier transformed during the linearization, are moved to the right hand side of the equations. In this manner, the left hand side resembles Eqs. (1). The resulting equations can be combined in order to obtain an equation for the variable $h \equiv \ln n$ as:

$$P\frac{\partial h}{\partial x} = G + G_t + G_y \tag{4}$$

where P and G are functions identical to the ones derived for the 1D model, and G_t and G_y are functions of the macroscopic variables and proportional to their time and azimuthal derivatives respectively.

Two equations from Eqs. (3) have special relevance. These are the azimuthal momentum equations for electrons and ions, which may be expressed as:

$$0 = -\frac{\partial}{\partial y}(nT_e) + en\frac{\partial\phi}{\partial y} + m_e n \nu_e (\chi v_{ex} - v_{ey}) \tag{5}$$

$$v_{ix}\frac{\partial v_{iy}}{\partial x} = -\nu_i (v_{iy} - v_{ny}) - \frac{\partial v_{iy}}{\partial t} - \frac{e}{m_i}\frac{\partial\phi}{\partial y} - v_{iy}\frac{\partial v_{iy}}{\partial y} \tag{6}$$

where v_{ny} and v_{iy} are the azimuthal neutral and ion velocities respectively, and the rest of symbols are as above.

Equation (5) reduces to the condition $v_{ey} = \chi v_{ex}$ in the axi-symmetric limit. However, if there are azimuthal gradients, this equation explains why correlated plasma density and electric field azimuthal oscillations may produce a net axial electron current. This can be seen by integrating Eq. (5) in the azimuthal direction to obtain the electron axial flux in terms of the electron azimuthal flux and the **E**x**B** drift coming from the electric field in the azimuthal direction.

Equation (6) has the peculiarity of defining another special point along the channel. In the point that separates the ionization region and the ion back-streaming region ($v_{ix} = 0$), this equation requires a regular transition. Thus the right hand side of the equation must be zero at that point as well. This fact has important consequences on the way the equations are solved.

C. Linearization

Equations (3) can be linearized around a steady-state and axi-symmetric solution (i.e., zero-th order background solution). To this end, it is possible to assume that a macroscopic variable $u(x, y, t)$ may be written as the sum of the zero-th order solution, $u_0(x)$, and a perturbation, $\tilde{u}_1(x, y, t)$. The small perturbations hypothesis ($\tilde{u}_1 \ll u_0$) allows linearizing Eqs. (3) and decouple the evolution of the zero-th order solution, which is given by Eqs. (1), from the evolution of the perturbations. These can be Fourier-expanded in t and y and, then, the complete solution may be expressed as:

$$u(x, y, t) = u_0(x) + \Re\left\{u_1(x; \omega, k) \exp(-i\omega t + iky)\right\} \tag{7}$$

where $\omega = \omega_r + i\omega_i$ is the angular frequency of the perturbation, being ω_r and ω_i its real and imaginary parts, and k is the azimuthal wave number of the perturbation. Note that k only admits a discrete number of values due to continuity conditions in the azimuthal direction, $k = m/R$, where m is the mode number and R is the mean radius of the thruster. Note as well that in order to consider consistently the axial gradients of the variables, the zero-th order solution and the coefficients of the Fourier expansion of the perturbations must retain the dependence on the axial coordinate. This is the main difference with respect to local stability analyses such as the one previously presented by the authors[48] .

Similarly, the perturbations of any control parameter (say, w) of the Hall discharge (voltage, mass flow, neutral velocity at the anode, and electron temperature at the cathode) may also be Fourier-expanded as:

$$w(t) = w_0 + \Re\left\{w_1 \exp(-i\omega t + iky)\right\} \tag{8}$$

where $w_0 \gg w_1$ is the condition for small perturbations.

It is possible to obtain a linear system of equations with variable coefficients describing the evolution of the different perturbations along the channel applying Eq. (7) to Eqs. (3). The resulting equations contain source terms proportional to the angular frequency, ω, and to the azimuthal wave number number, k, of the perturbation. These equations must be solved several times, once for each fundamental mode associated to the boundary conditions. Moreover, the zero-th order solution must also be solved together with the perturbation problem in order to be able to compute the coefficients of the perturbation equations.

The boundary conditions associated to the evolution equations are also derived linearizing the boundary conditions of the one dimensional problem. The result of this linearization has already been proposed by Ahedo *et al.*[45]

D. Solution method and self-excited modes

The presence of a sonic point and of a zero-ion-velocity point inside the thruster channel makes the integration process cumbersome. The solution is computed by concatenating the fundamental modes obtained integrating the equations from the anode and from those two special points. Obviously, the solution must be continuous in some intermediate points and this imposes additional constraints to the final solution. Additional initial conditions are necessary so that the integration can be started from the anode and those two special points. In the end, the value of the weights of the fundamental modes of the final solution are obtained from the following system of equations:

$$A\vec{x} = \vec{b} \tag{9}$$

where $\vec{x}$ is a vector containing the weights of the fundamental modes, $\vec{b}$ is a vector with the coefficients of the linearized control parameters and constraints and A is a matrix with complex coefficients containing the partial derivatives of the control parameters with respect to the initial conditions of each of the fundamental modes. This matrix A depends on the control parameters of the zero-th order solution, w_0, as well as the angular frequency, ω, and the wave number, k, of the perturbation, that is, $A = A(w_0, \omega, k)$.

In order to have self-excited modes, the previous algebraic system of equations must have non-trivial solutions for the homogeneous problem (i.e., case with $\vec{b} = 0$). This condition is equivalent to:

$$\det A(w_0, \omega, k) = 0. \tag{10}$$

where det is the determinant function.

For each zero-th order solution given by the control parameters, w_0, and each wave number, k, Eq. (10) provides a condition to compute the complex angular frequency, ω, of the perturbation. If the resulting angular frequency verifies the condition $\omega_i > 0$, then the perturbation is self-excited. In particular, the case $k = 0$ corresponds to axial oscillations studied in the past for the analysis of the breathing mode[45–47] .

E. Anomalous diffusion and azimuthal oscillations

The formulation presented so far has mostly focused on the analysis of the linear stability of the Hall discharge against azimuthal perturbations. In case a self-excited oscillation is detected then unstable oscillations grow and eventually saturate. The linear growth phase is the only one modelled with the 2D model presented here while the saturation is a non-linear process. Anomalous diffusion is related to that non-linear process and cannot be determined self-consistently here. Nonetheless, some insight can be obtained. To this end, it will be assumed that the *shape* of the saturated oscillations is given by the solution of the first order problem presented above. This is incorrect as the linear formulation is only valid as long as the perturbations are small compared to the background solution, whereas the oscillations only saturate when their size is comparable to the zero-th order solution. Nevertheless, let us continue along this not so consistent path.

Let us define the azimuthal average of a function $z(t,x,y)$ as $\langle z\rangle(t,x)$ and recall that it is possible to express:

$$z(t,x,y) = \langle z\rangle(t,x) + \hat{z}(t,x,y) \qquad \text{where} \qquad \langle \hat{z}\rangle \equiv 0 \tag{11}$$

If we obtain the azimuthal average of the azimuthal electron momentum equation in Eq. (5), then we obtain the following expression:

$$\langle n v_{ex}\rangle = \frac{m_e}{eB}\langle \nu_e n v_{ey}\rangle + \frac{\langle n_1 E_{y1}\rangle}{B} \tag{12}$$

where the magnetic field has been assumed to be axi-symmetric ($\partial B/\partial y = 0$). The previous expression can be further expanded to better identify the different terms in the following way:

$$\langle n_1 v_{ex1}\rangle = \frac{\nu_{e0}}{\omega_e}\langle n_1 v_{ey1}\rangle + \frac{1}{\omega_e}\left(\langle \nu_{e1} n_1\rangle v_{ey0} + n_0\langle \nu_{e1} v_{ey1}\rangle\right) + \frac{\langle n_1 E_{y1}\rangle}{B} \tag{13}$$

where E_{y1} is the perturbed azimuthal electric field, ω_e is the electron cyclotron frequency, and it has been used that $\langle n v_{ex}\rangle = n_0 v_{ex0} + \langle n_1 v_{ex1}\rangle$ and $v_{ey0} = \chi_0 v_{ex0}$. Equation (13) shows the additional axial electron flux caused by the oscillations as the combination of different terms. The second and third terms of the right-hand side of Eq. (13) correspond to the additional flux from the perturbed collisionality caused by the oscillations. Finally, the last term corresponds to the flux coming from the **E**x**B** drift caused by the azimuthal electric field oscillation. This last term is suspected to be the source of the Bohm diffusion as the other are collisional terms and are expected to be much smaller. If we retain only the azimuthal electric field term, then it is possible to write:

$$\langle n v_{ex}\rangle = \frac{\nu_e'}{\omega_e}\langle n v_{ey}\rangle \qquad \text{where} \qquad \nu_e' = \nu_e + \omega_e \frac{\langle n_1 E_{y1}\rangle/B}{\langle n v_{ey}\rangle} \tag{14}$$

If we now obtain the azimuthal average of the axial electron momentum equation in Eqs. (3), then it is possible to write:

$$0 = -e\langle n E_x\rangle - \frac{\partial}{\partial x}\langle n T_e\rangle - m_e\omega_e\langle n v_{ey}\rangle \tag{15}$$

where the collisional term $\nu_e n v_{ex}$ has been neglected as $\nu_e \ll \omega_e$ and $v_{ex} \ll v_{ey}$. The combination of the last two expressions yields:

$$0 = -e\langle n E_x\rangle - \frac{\partial}{\partial x}\langle n T_e\rangle - m_e\frac{\omega_e^2}{\nu_e'}\langle n v_{ex}\rangle \tag{16}$$

Equation (16) resembles the evolution equation of the 1D model of Ahedo *et al.*. However, it includes non-linear oscillatory terms such as $\langle n_1 E_{x1}\rangle$. If we assume that the only relevant non-linear term is the one associated to the azimuthal electric field, then:

$$0 = en_0\frac{\partial \phi_0}{\partial x} - \frac{\partial}{\partial x}\left(n_0 T_{e0}\right) - m_e\frac{\omega_e^2}{\nu_e'} n_0 v_{ex0} \quad \text{where} \quad \nu_e' = \nu_e + \omega_e\frac{\langle n_1 E_{y1}\rangle/B}{n_0 v_{ey0}} \tag{17}$$

The last expression resembles the definition of the Bohm diffusion frequency ($\nu_B = \alpha_B\omega_e$). In fact, it is possible to establish the following relationship:

$$\alpha_B(x) = \frac{\langle n_1 E_{y1}\rangle/B}{n_0 v_{ey0}} \tag{18}$$

Given the perturbations of plasma density and azimuthal electric field, Eq. (18) allows obtaining the equivalent anomalous diffusion coefficient associated to the perturbations.

III. Results and discussion

A. Reference case and background solution

This section is devoted to the presentation of the results of the linearized time-dependent 2D model for typical Hall thruster conditions. For this purpose, a SPT-100 model has been considered as reference case. The main operating parameters of this reference case used in this simulation are presented in Table 1.

Table 1. Main operating parameters of the SPT-100 Hall Thruster used as reference case for the simulations.

$\dot{m}$	4.85 mg/s	V_d	300 V
B_{max}	237 G	x_{max}	20 mm
L_{ch}	25 mm	L_{AE}	33 mm
h_c	15 mm	R	42.5 mm
T_{eE}	4.8 eV	v_{nB}	300 m/s
α_B	0.01	$\tilde{\nu}_w$	0.16
T_{SEE}	100 V	a_w	1.0
T_{eB}	1.2 eV	I_d	5.00 A

where $\dot{m}$ is the mass flow rate through the anode, V_d is the discharge potential, B_{max} is the maximum magnetic field, x_{max} is the location of the maximum magnetic field with respect to the anode, L_{AE} is the distance from anode to external cathode, L_{ch} is the length of the channel, h_c is the width of the channel, R is the mean radius of the channel, T_{eE} is the cathode temperature, v_{nB} is the neutral velocity at injection, α_B is the anomalous diffusion coefficient, $\tilde{\nu}_w$ is a dimensionless coefficient for the wall losses model[12] , T_{SEE} is the electron temperature yielding 100% of secondary electron emission for the wall material and is used for the wall losses model, a_w is the accommodation factor for wall recombination, T_{eB} is the electron temperature at the the anode, and I_d is the discharge current, being the last two variables outputs of the simulation.

Figure 1 shows the axial profiles of the main macroscopic variables corresponding to the background solution of Eqs. (1) for the reference case described in Table 1.

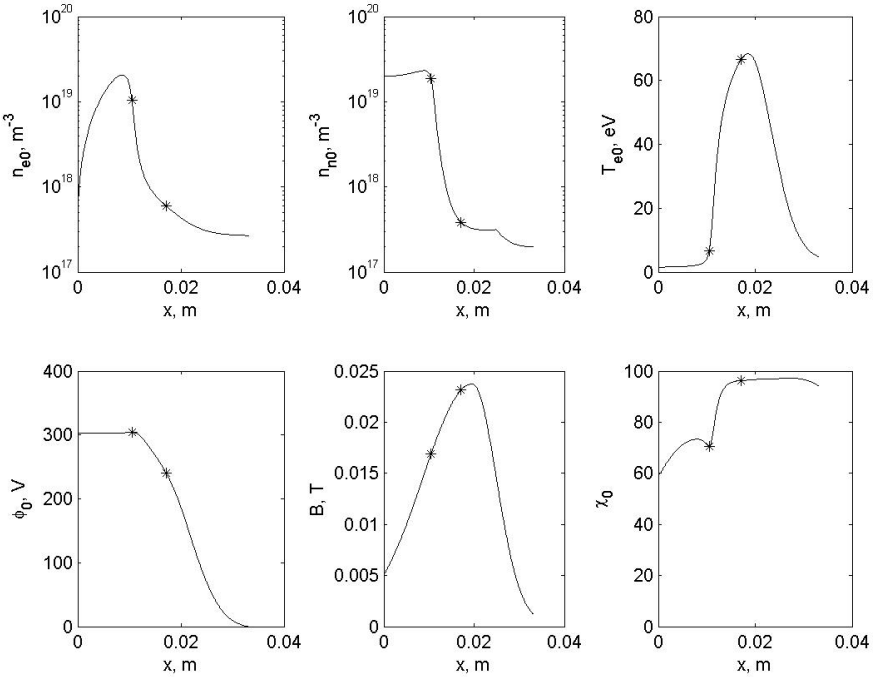

Figure 1. Axial profiles of main macroscopic variables of the background solution for the reference case: x is the axial location, n_{e0} is the plasma density, n_{n0} is the neutral density, T_{e0} is the electron temperature, ϕ_0 is the electric potential, B is the magnetic field and χ_0 is the Hall parameter. In each plot, the left asterisk corresponds to the zero-ion-velocity point whereas the right asterisk corresponds to regular sonic point inside the channel. The space between both points corresponds roughly to the ionization region of the thruster.

B. Azimuthal oscillations

As a result of the global stability analysis of the reference case described in Table 1, a self-excited oscillation is detected with an azimuthal mode number $m = -1$, where $m = Rk_y$, a frequency $f = 11.1$ kHz, and a growth-rate $\omega_i/2\pi \approx 3$ kHz. Based on these values, the azimuthal oscillation has properties similar to those experimentally observed for the spoke. As it will be shown later, its growth rate is similar to the corresponding one for the breathing mode ($m = 0$). Thus, it is not clear from this analysis which oscillation, the azimuthal one or the axial one, dominates in the reference case.

It must be noted that other mode numbers ($m = -2$, $m = +1$ or $m = +2$) have been evaluated as part the of global stability analysis looking for possible self-excited solutions. However, for the reference case under consideration the only mode numbers resulting in self-excited solutions are $m = 0$ (breathing mode) and $m = -1$ (spoke). This is in line with experimental results for normal-size thrusters, where the spoke is normally detected as a single oscillation in the azimuthal direction. In the case of larger thrusters, experiments show that higher modes ($m = -2, -3, -4$) might become dominant[25] . However, the scaling of the azimuthal oscillations shown here to bigger thrusters has not been investigated in the current study.

Figure 2 shows the contour maps in the $x - t$ space (at $y = 0$) of the main macroscopic variables as combinations of the background solution and the perturbations for the self-excited oscillation mentioned above. As the size of the perturbations does not result from the linear perturbations problem, it must be chosen arbitrarily. This size has been selected so that the maximum electron temperature perturbation is 100% of the background electron temperature at the same location. Obviously, this size is outside the range of validity of the linear approximation, but allows representing more clearly the oscillations. This is justified as typical spoke oscillations have a size of similar magnitude as the average value. A side effect of this selection is that some macroscopic variables can reach non-physical values (e.g., negative temperature or negative density). In reality, before these non-physical values are reached non-linear effects start playing a role and make the oscillation non-linear. Moreover, the growth of the oscillations over time is not represented in the plots.

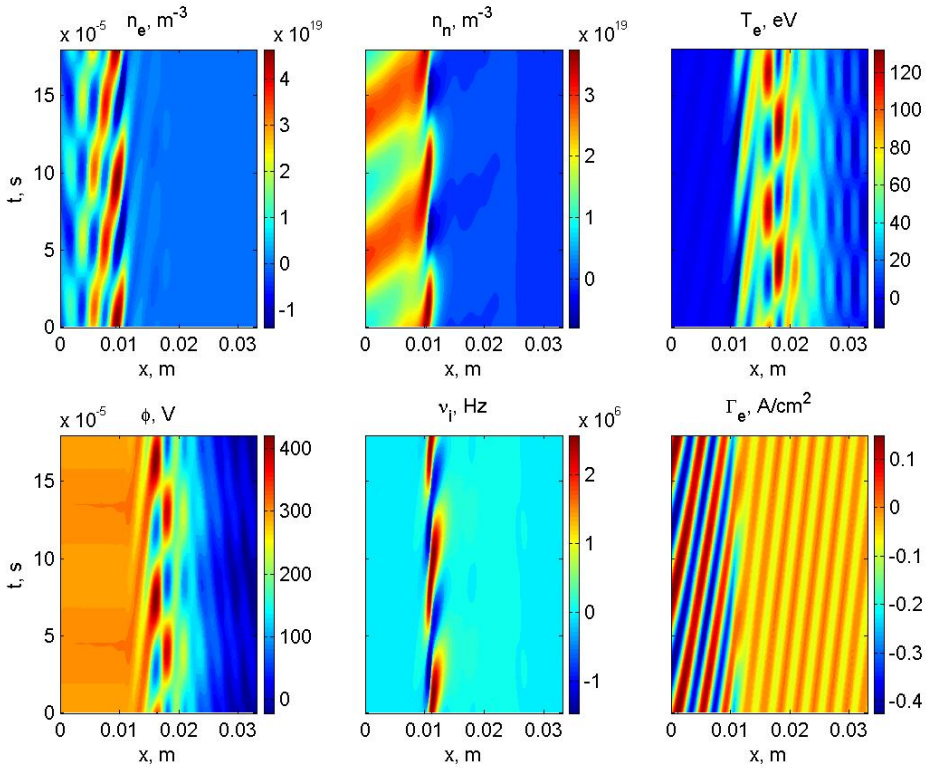

Figure 2. Oscillations of the main macroscopic variables as combinations of the background solution and the perturbations shown as functions of x and t at $y = 0$ for a self-excited unstable oscillation of the perturbation problem for the reference case presented in Table 1. The azimuthal mode number is $m = -1$, the frequency is $f = 11.1$ kHz and the growth-rate is $\omega_i/2\pi \approx 3$ kHz. Variables represented (from left to right and upper to lower): plasma density, n_e; neutral density, n_n; electron temperature, T_e; electric potential, ϕ; ionization frequency, ν_i; electron axial flux, Γ_e.

Figure 3 shows contour maps in the $x-y$ space for different instants of time, t, during one cycle of the azimuthal oscillation. In this figure, it is possible to observe how the oscillation travels in the $-y$ direction, this is, in the **E**x**B** direction. As expected, the same patterns shown in Fig. 2 are observed in Fig. 3 moving in the azimuthal direction.

According to Fig. 3, the azimuthal oscillation is due to an azimuthal variation of the ionization. The connection between the spoke oscillation and the ionization process had already been suggested theoretically by the authors[35,48] and, based on experiments, by other researchers.[49] This fact is further analysed in the next section, where the azimuthal oscillation is compared against the breathing mode.

It is also interesting to point out that the perturbed electric field has a roughly constant azimuthal component upstream of the ionization region (see fourth row of Fig. 3). This fact, together with the plasma density variation, causes a net axial electron current to the anode coming from the **E**x**B** drift in the axial direction, as can be observed in the last row of plots of Fig. 3.

Another important aspect to mention is the large relative size of temperature and electric potential oscillations in the narrow ionization region. The reason for the ionization region being so narrow resides in the fact that heat conduction effects are not considered in the model. The version of the 1D model of Ahedo that takes into consideration heat conduction terms[42] gives smoother temperature profiles, wider ionization regions and lower temperatures inside the thruster. These facts could help in reducing the relative size of the temperature and electric potential oscillations.

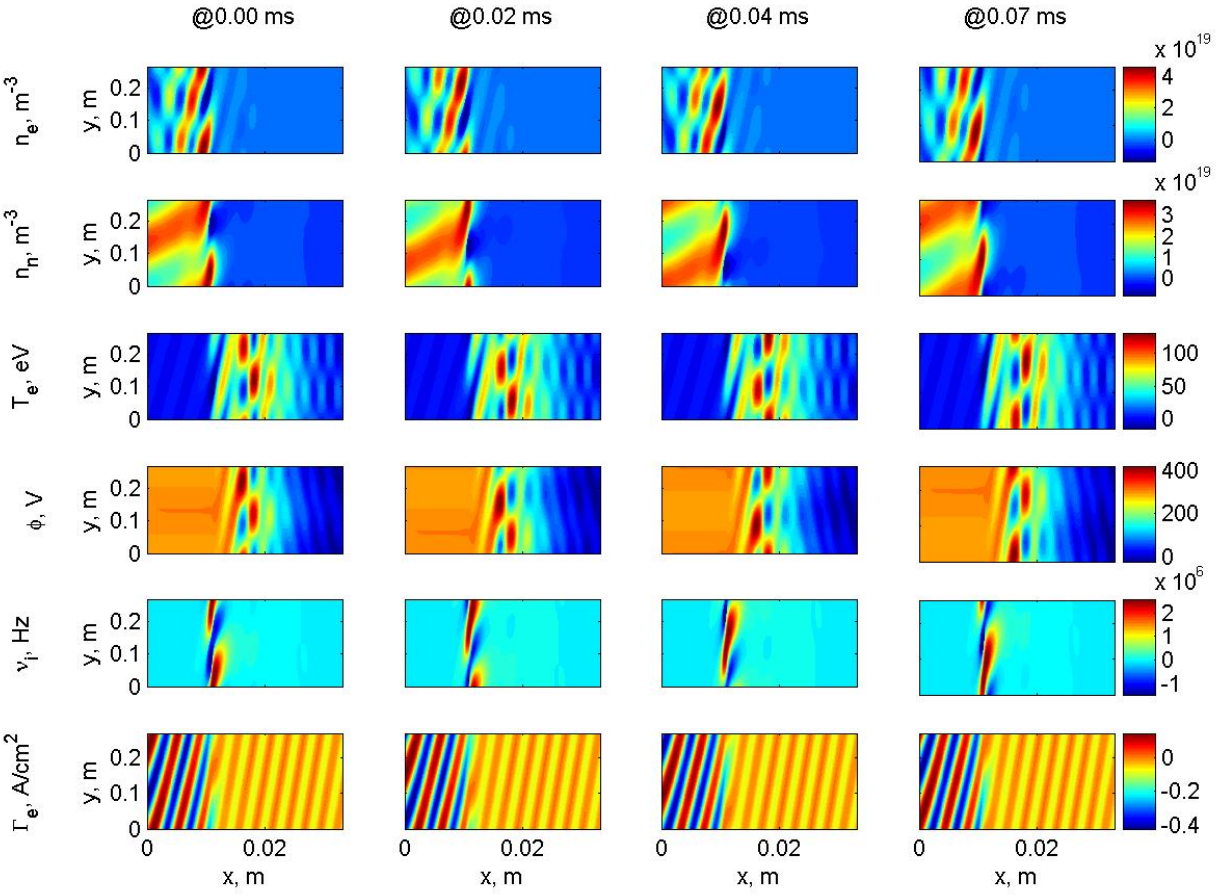

Figure 3. Oscillations of the main macroscopic variables as combinations of the background solution and the perturbations shown as functions of x and y at different values of t (@ t ms) for the same conditions used previously in Fig. 2. Variables represented (from upper to lower): plasma density, n_e; neutral density, n_n; electron temperature, T_e; electric potential, ϕ; ionization frequency, ν_i; electron axial flux, Γ_e.

For completeness, Fig. 4 shows the axial profiles of the complex coefficients of the Fourier-expansion of the perturbations of Eq. (7). These are the variables resulting from the integration process of the linearized equations.

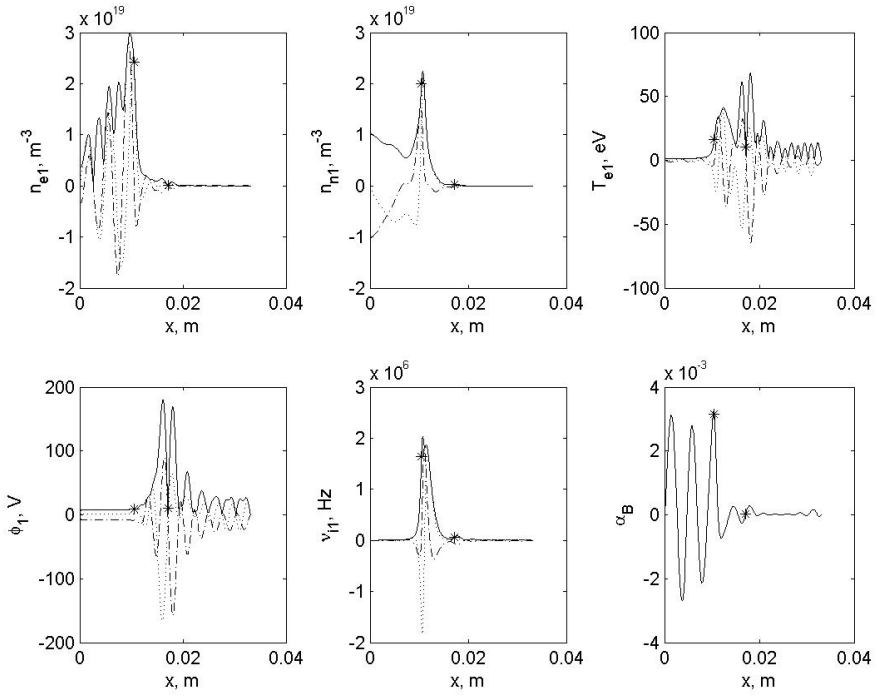

Figure 4. Axial profiles of the coefficients of the Fourier-expanded perturbations of the main macroscopic variables corresponding to a self-excited unstable oscillation of the perturbation problem for the reference case presented in Table 1 and the same conditions as in Fig. 2. Variables represented: x is the axial location, n_{e1} is the perturbation of the plasma density, n_{n1} is the perturbation of the neutral density, T_{e1} is the perturbation of the electron temperature, ϕ_1 is the perturbation of the electric potential, ν_{i1} is the perturbation of the ionization frequency, and α_B is the equivalent anomalous diffusion coefficient derived from the linear oscillations. Dotted lines are used for the real part of the perturbation coefficient, dash-dotted lines are used for the imaginary part and continuous lines are used for the modulus of the perturbation coefficient.

C. Parametric continuation

As starting point for the parametric continuation the same case as described in Table 1 is used, except that this time wall losses are not accounted for. Under these reference conditions, the mode $m = -1$ has a growth rate five times larger than the $m = 0$ mode and thus, the spoke oscillation dominates over the breathing mode. The parameter that is modified as part of the parametric variation is the discharge voltage together with the magnetic field. In all cases, the mode number is kept constant at $m = -1$ together with the rest of operating parameters such as the mass flow rate or the electron cathode temperature.

Table 2 shows the variation of the frequency, f, and growth rate, $\omega_i/2\pi$, of the azimuthal oscillation with the discharge potential, V_d, and the maximum magnetic field, B_{max}. The frequency increases with V_d whereas the growth rate decreases. Experimental results[26] show also the increase of the oscillation frequency with the discharge voltage. Moreover, the spoke oscillation tends to become less important when operating the thrusters at high voltage in the current-saturated part of the I-V curve,[16] what is coherent with the decrease in the growth rate of the oscillation with the discharge voltage reported here.

Table 2. Variation of the frequency, f, and growth rate, $\omega_i/2\pi$, of the azimuthal oscillation with the discharge voltage and the maximum magnetic field.

V_d, V	B_{max}, G	f, kHz	$\omega_i/2\pi, kHz$
300	237	12.5	13.3
333	265	22.7	0.6
366	294	26.5	-8.7

D. Comparison with the breathing mode

Similarly to Fig. 2, Fig. 5 shows the contour maps in the $x-t$ space of the main variables for an unstable oscillation with $m = 0$ for the case presented in Table 1. The frequency at which the oscillation is unstable is $f = 9.1$ kHz whereas the growth-rate is $\omega_i/2\pi \approx 3$ kHz. The frequency of the simulated breathing mode is smaller than for the azimuthal oscillation presented previously, as normally observed in experiments[15,19] .

In the azimuthal oscillation (see Fig. 2), the ionization front moves back and forth, as in the breathing mode (see Fig. 5). Moreover, at a fixed axial and azimuthal location, the azimuthal oscillation also shows a standing wave of plasma density and a travelling wave of neutral density, as for the breathing mode. The similarity with the breathing mode, thus, seems clear and the fact that both modes are recovered with the very same model reinforces this idea. Moreover, the differences between both modes, apart from the azimuthal variation in the case with $m = -1$, are not obvious in terms of instability of the ionization process and the presence of travelling waves.

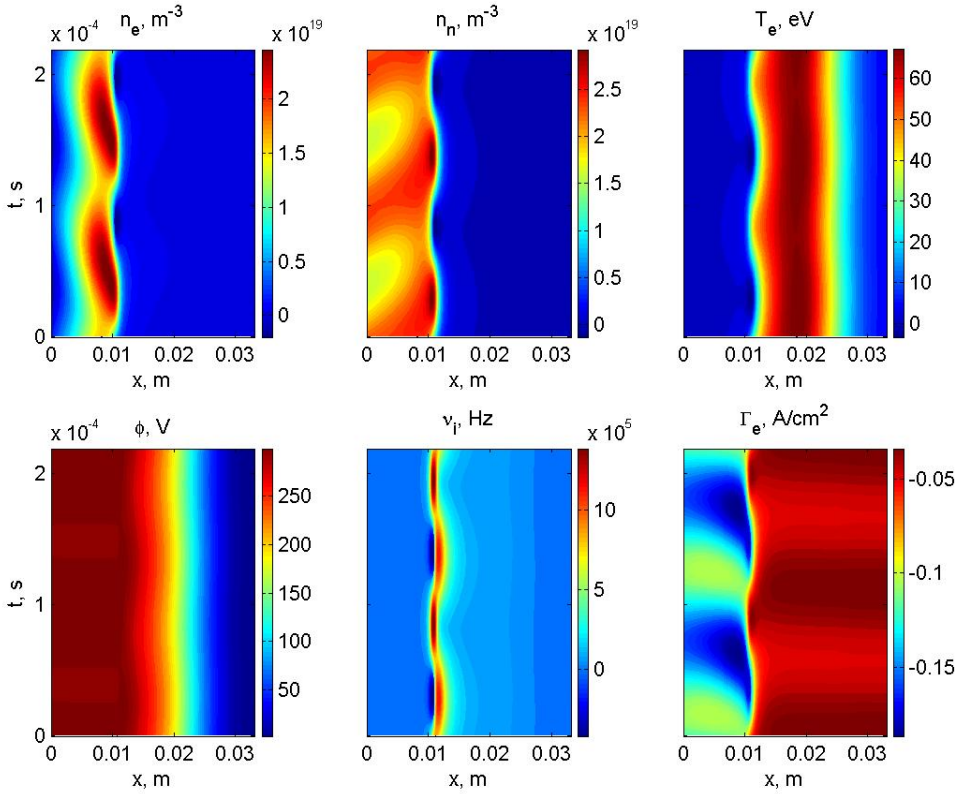

Figure 5. Oscillations as a function of x and t for the breathing mode ($m = 0$). The conditions and variables represented are similar to those shown in 2

Another interesting property common to both oscillations is the non-uniformity (in space and time) of the neutral density at the anode plane. This seems in contradiction with the imposed anode boundary conditions that enforce uniform neutral velocity and mass flow rate. The reason for the neutral density being non-uniform at the anode resides in the neutral recombination at the back wall of the thruster. This may be one of the reasons why the breathing mode and the spoke oscillation are unstable as it is explained next. Part of the ions generated in the ionization region are attracted to the anode through the ion-backstreaming region and are recombined into neutrals. These neutrals travel downstream and are available for subsequent ionization cycles, and thus, more ions are generated than in previous ionization cycles and sent back to the anode. The complete process is repeated again and, hence, the growing character of this mechanism.

In order to validate the previous mechanism, the following numerical test has been carried out. The boundary condition for neutral recombination at the anode has been relaxed in such a way that ions reaching the anode are not recombined to neutrals, but lost. Under these unrealistic boundary conditions, the growth rate of the breathing mode oscillation for the reference case is reduced by a factor greater than 2. Thus, it is verified numerically that the neutral recombination process promotes the instability of the breathing mode.

E. Anomalous diffusion

One of the consequences of the azimuthal oscillation is the enhanced electron conductivity inside the channel as observed in Fig. 3. In order to evaluate the net effect on the electron current, it is convenient to compute the equivalent anomalous diffusion coefficient, $\alpha_B(x)$, associated to the linear perturbations. This computation is shown in the last plot of Fig. 4 based on Eq. (18). That last plot shows the axial variation of $\alpha_B(x)$ averaged over time and azimuth. It is possible to observe that the net effect of the oscillation on the electron conductivity is concentrated in the rear part of the thruster, in the ion-backstreaming region. The values reached by $\alpha_B(x)$ in this region are of the same order of magnitude to that used for α_B in the simulation of the background solution of the reference case (see Table 1). However, this is only true for the selected size of linear oscillations that, as mentioned above, is such that the maximum temperature perturbation is 100% of the background temperature.

Another relevant aspect is the fact that $\alpha_B(x)$ reaches negative values in some regions of the channel. This is due to the change of phase between the plasma density and the azimuthal electric field perturbations that induce electron current to and away from the anode. In any case, for the case under analysis the average value of $\alpha_B(x)$ is positive although smaller than the peaks observed in Fig. 4. Moreover, the large variations of $\alpha_B(x)$ anticipate important changes in the background solutions, where α_B is considered constant, in case the profile of $\alpha_B(x)$ is used in the computation of the background. This is something that needs to be further investigated.

Furthermore, no contribution to electron conductivity is seen downstream the ionization region, where experiments also show a higher-than-expected electron mobility. Non-linear effects affecting the low-frequency azimuthal oscillation might resolve this contradiction. Another possible explanation is that high-frequency oscillations[50] (1-10 MHz) might play an important role in that region.

IV. Conclusions

A linearized time-dependent 2D model has been used for the analysis of the global stability of the Hall discharge. Contrary to more widely used local analyses, this approach takes into account consistently the axial variation of the plasma variables. Results show an unstable self-excited azimuthal oscillation travelling in the **E**x**B** direction with a mode number $m = -1$ and a frequency around 11 kHz. These features are similar to those experimentally observed for the so-called spoke. The analysis of the oscillation and the comparison with the breathing mode reveal that the ionization is the main driver for the azimuthal variation of the plasma and neutral densities. Moreover, estimates of the electron conductivity caused by the azimuthal oscillation show a relevant contribution in the rear part of the thruster. However, in the acceleration region this oscillation does not seem to impact the electron mobility. Additionally, a parametric variation shows that the frequency of the oscillation increases when the discharge voltage decreases, whereas its growth rate decreases. These two trends are also found in experiments.

As part of future work to be carried out, aside from additional parametric analyses to understand how the azimuthal oscillation scales with different operating parameters, we identify more areas of research. Firstly, a comparison between the stability criteria derived from local stability analyses[29–31,35] and the results from the global stability. This can be achieved by analyzing the local stability of the axial profiles of the reference case and compare the results against the ones presented here. This comparison should allow us to identify the local stability analysis that best matches the global one, if any. Secondly, we intend to extend the linearized time-dependent 2D model to high frequency (1-10 MHz) so that electron drift oscillations[50] in the azimuthal direction can be analysed numerically. This analysis would continue the theoretical analyses already carried out in previous studies[36,39] . Thirdly, the inclusion of heat conduction effects in the model might help in widening the ionization region and smoothing the temperature profile as in the current simulations it is too steep. And finally, another aspect to be studied is the use of the profile of the equivalent anomalous diffusion coefficient, $\alpha_B(x)$, derived from the linear oscillations in the computation of the background solution.

Acknowledgments

Support is being provided by the Air Force Office of Scientific Research, Air Force Material Command, USAF, under Grant No. FA8655-13-1-3033. Additional support comes from Spain's R&D National Plan (Proyect AYA-2010-61699)

References

[1]A. Morozov, Y. Esipchuk, G. Tilinin, A. Trofimov, and Y. Sharov, "Plasma accelerator with closed electron drift and extended acceleration zone," *Soviet Physics-Tech. Physics*, vol. 17, no. 1, pp. 38–45, 1972.

[2]N. Meezan and M. Cappelli, "Electron density measurements for determining the anomalous electron mobility in a coaxial Hall discharge plasma," in *Proceedings of the 36th Joint Propulsion Conference*, 2000.

[3]J. A. Linnell and A. D. Gallimore, "Hall Thruster Electron Motion Characterization Based on Internal Probe Measurements," in *Proceedings of the 31st International Electric Propulsion Conference*, 2009.

[4]N. Meezan, W. Hargus Jr, and M. Cappelli, "Anomalous electron mobility in a coaxial Hall discharge plasma," *Physical Review E*, vol. 63, no. 2, p. 26410, 2001.

[5]M. Cappelli, N. Meezan, and N. Gascon, "Transport physics in Hall plasma thrusters," in *Proceedings of the 40th AIAA Aerospace and Sciences Meeting and Exhibit*, 2002.

[6]C. Boniface, L. Garrigues, G. Hagelaar, J. Boeuf, D. Gawron, and S. Mazouffre, "Anomalous cross field electron transport in a Hall effect thruster," *Applied Physics Letters*, vol. 89, p. 161503, 2006.

[7]D. Gawron, S. Mazouffre, and C. Boniface, "A Fabry–Pérot spectroscopy study on ion flow features," *Plasma Sources Science and Technology*, vol. 15, pp. 757–764, 2006.

[8]A. Morozov, Y. Esipchuk, A. Kapulkin, V. Nevrovskii, and V. Smirnov, "Effect of the magnetic field on a closed-electron-drift accelerator," *Soviet Physics-Tech. Physics*, vol. 17, no. 3, pp. 482–487, 1972.

[9]S. Yoshikawa and D. Rose, "Anomalous diffusion of a plasma across a magnetic field," *Physics of Fluids*, vol. 5, p. 334, 1962.

[10]G. Janes and R. Lowder, "Anomalous Electron Diffusion and Ion Acceleration in a Low-Density Plasma," *Physics of Fluids*, vol. 9, p. 1115, 1966.

[11]A. Morozov, "Conditions for efficient current transport by near-wall conduction," *Sov. Phys. Tech. Phys*, vol. 32, no. 8, pp. 901–904, 1987.

[12]E. Ahedo, J. Gallardo, and M. Martinez-Sanchez, "Effects of the radial plasma-wall interaction on the hall thruster discharge," *Physics of Plasmas*, vol. 10, p. 3397, 2003.

[13]L. Garrigues, G. Hagelaar, C. Boniface, and J. Boeuf, "Anomalous conductivity and secondary electron emission in Hall effect thrusters," *Journal of Applied Physics*, vol. 100, p. 123301, 2006.

[14]F. Parra, E. Ahedo, J. Fife, and M. Martinez-Sanchez, "A two-dimensional hybrid model of the Hall thruster discharge," *Journal of Applied Physics*, vol. 100, p. 023304, 2006.

[15]E. Choueiri, "Plasma oscillations in Hall thrusters," *Physics of Plasmas*, vol. 8, p. 1411, 2001.

[16]Y. Esipchuk, A. Morozov, G. Tilinin, and A. Trofimov, "Plasma oscillations in closed-drift accelerators with an extended acceleration zone," *Sov. Physics-Tech. Physics*, vol. 18, no. 7, pp. 928–932, 1974.

[17]P. Lomas and J. Kilkenny, "Electrothermal instabilities in a Hall accelerator," *Plasma Physics*, vol. 19, p. 329, 1977.

[18]W. A. Hargus, N. B. Meezan, and M. A. Cappelli, "A study of a low power hall thruster transient behavior," in *Proceedings of the 25th International Electric Propulsion Conference*, pp. 351–358, 1997.

[19]E. Chesta, C. Lam, N. Meezan, D. Schmidt, and M. Cappelli, "A characterization of plasma fluctuations within a Hall discharge," *IEEE transactions on Plasma science*, vol. 29, no. 4, pp. 582–591, 2001.

[20]N. Gascon and M. Cappelli, "Plasma instabilities in the ionization regime of a Hall thruster," in *Proceedings of the 29th Joint Propulsion Conference*, 2003.

[21]A. Smith and M. Cappelli, "Time and Space-correlated Plasma Property Measurements in the Near-field of a Coaxial Hall Discharge," in *Proceedings of the 31st International Electric Propulsion Conference*, 2009.

[22]Y. Raitses, A. Smirnov, and N. Fisch, "Effects of enhanced cathode electron emission on hall thruster operation," *Physics of Plasmas*, vol. 16, p. 057106, 2009.

[23]J. Parker, Y. Raitses, and N. Fisch, "Transition in electron transport in a cylindrical hall thruster," *Applied Physics Letters*, vol. 97, p. 091501, 2010.

[24]C. Ellison, Y. Raitses, and N. Fisch, "Fast camera imaging of hall thruster ignition," *IEEE Transactions on Plasma Science*, vol. 39, no. 11, pp. 2950–2951, 2011.

[25]M. S. McDonald and D. Gallimore, A, "Parametric Investigation of the Rotating Spoke Instability in Hall Thrusters," in *Proceedings of the 32nd International Electric Propulsion Conference*, 2011.

[26]D. Liu, *Two-Dimensional Time-Dependent Plasma Structures of a Hall-Effect Thruster*. PhD thesis, Standford University, 2011.

[27]Y. Esipchuk and G. Tilinin, "Drift instability in a Hall-current plasma accelerator," *Sov. Physics-Tech. Physics*, vol. 21, no. 4, pp. 417–423, 1976.

[28]A. Kapulkin and M. Guelman, "Low Frequency Instability and Enhanced Transfer of Electrons in Near-Anode Region of Hall Thruster," in *Proceedings of the 30th International Electric Propulsion Conference*, 2007.

[29]A. Kapulkin and M. M. Guelman, "Low-frequency instability in near-anode region of hall thruster," *IEEE Transactions on Plasma Science*, vol. 36, no. 5, pp. 2082–2087, 2008.

[30]W. Frias, A. I. Smolyakov, I. D. Kaganovich, and Y. Raitses, "Long wavelength gradient drift instability in hall plasma devices. i. fluid theory," *Physics of Plasmas*, vol. 19, p. 072112, 2012.

[31]A. Smolyakov, W. Frias, Y. Raitses, and N. J. Fisch, "Gradient instabilities in Hall thruster plasmas," in *Proceedings of the 32nd International Electric Propulsion Conference*, 2011.

[32]E. Chesta, N. Meezan, and M. Cappelli, "Stability of a magnetized Hall plasma discharge ," *Journal of Applied Physics*, vol. 89, no. 6, pp. 3099–3107, 2001.

[33]J. Gallardo and E. Ahedo, "On the anomalous diffusion mechanism in Hall-effect thrusters," in *Proceedings of 29th International Electric Propulsion Conference*, 2005.

[34]H. K. Malik and S. Singh, "Resistive instability in a hall plasma discharge under ionization effect," *Physics of Plasmas*, vol. 20, p. 052115, 2013.

[35]D. Escobar and E. Ahedo, "Low frequency azimuthal stability of the ionization region of the hall thruster discharge. i. local analysis," in *To be submitted*.

[36]A. Litvak and N. Fisch, "Rayleigh instability in Hall thrusters," *Physics of Plasmas*, vol. 11, p. 1379, 2004.

[37]A. Kapulkin and V. Prisnyakov, "Dissipative method of suppression of electron drift instability in SPT," in *Proceedings of the 24th International Electric Propulsion Conference*, 1995.

[38]A. Kapulkin, J. Ashkenazy, A. Kogan, G. Appelbaum, D. Alkalay, and M. Guelman, "Electron instabilities in Hall thrusters: modelling and application to electric field diagnostics," in *Proceedings of the 28th International Electric Propulsion Conference*, 2003.

[39]A. Kapulkin and M. Guelman, "Lower-hybrid instability in Hall thruster," in *Proceedings of the 29th International Electric Propulsion Conference*, 2005.

[40]H. K. Malik and S. Singh, "Conditions and growth rate of rayleigh instability in a hall thruster under the effect of ion temperature," *Physical Review E*, vol. 83, no. 3, p. 036406, 2011.

[41]E. Ahedo, P. Martinez-Cerezo, and M. Martinez-Sanchez, "One-dimensional model of the plasma flow in a Hall thruster," *Physics of Plasmas*, vol. 8, p. 3058, 2001.

[42]E. Ahedo, J. Gallardo, and M. Martinez-Sanchez, "Model of the plasma discharge in a hall thruster with heat conduction," *Physics of Plasmas*, vol. 9, p. 4061, 2002.

[43]E. Ahedo and D. Escobar, "Influence of design and operation parameters on hall thruster performances," *Journal of applied physics*, vol. 96, p. 983, 2004.

[44]E. Ahedo and F. Parra, "A model of the two-stage hall thruster discharge," *Journal of applied physics*, vol. 98, p. 023303, 2005.

[45]E. Ahedo, P. Martinez, and M. Martinez-Sanchez, "Steady and linearly-unsteady analysis of a hall thruster with an internal sonic point," *AIAA paper*, vol. 3655, 2000.

[46]R. Noguchi, M. Martinez-Sanchez, and E. Ahedo, "Linear 1-d analysis of oscillations in hall thrusters," in *Proceedings of the 26th International Electric Propulsion Conference*, 1999.

[47]S. Barral, V. Lapuerta, A. Sancho, and A. E, "Numerical investigation of low-frequency longitudinal oscillations in Hall thrusters," in *Proceedings of the 29th International Electric Propulsion Conference*, 2005.

[48]D. Escobar and E. Ahedo, "Ionization-induced azimuthal oscillation in Hall Effect Thrusters," in *Proceedings of the 32nd International Electric Propulsion Conference*, 2011.

[49]A. Vesselovzorov, E. Dlougach, E. Pogorelov, A.A. Svirskiy, and V. Smirnov, "Low-frequency wave experimental investigations, transport and heating of electrons in stationary plasma thruster SPT," in *Proceedings of the 32nd International Electric Propulsion Conference*, 2011.

[50]A. Lazurenko, V. Krasnoselskikh, and A. Bouchoule, "Experimental Insights Into High-Frequency Instabilities and Related Anomalous Electron Transport in Hall Thrusters," *IEEE Transactions on Plasma Science*, vol. 36, no. 5 Part 1, pp. 1977–1988, 2008.